

Beyond Master and Apprentice: Grounding Foundation Models for Symbiotic Interactive Learning in a Shared Latent Space

Linus Nwankwo*; Björn Ellensohn; Christian Rauch; Elmar Rueckert

Abstract—Today’s autonomous agents can understand free-form natural language instructions and execute long-horizon tasks in a manner akin to human-level reasoning. These capabilities are mostly driven by large-scale pre-trained foundation models (FMs). However, the approaches with which these models are grounded for human-robot interaction (HRI) perpetuate a master-apprentice model, where the apprentice (embodied agent) passively receives and executes the master’s (human’s) commands without reciprocal learning. This reactive interaction approach does not capture the co-adaptive dynamics inherent in everyday multi-turn human-human interactions. To address this, we propose a Symbiotic Interactive Learning (SIL) approach that enables both the master and the apprentice to co-adapt through mutual, bidirectional interactions. We formalised SIL as a co-adaptation process within a shared latent task space, where the agent and human maintain joint belief states that evolve based on interaction history. This enables the agent to move beyond reactive execution to proactive clarification, adaptive suggestions, and shared plan refinement. To realise these novel behaviours, we leveraged pre-trained FMs for spatial perception and reasoning, alongside a lightweight latent encoder that grounds the models’ outputs into task-specific representations. Furthermore, to ensure stability as the tasks evolve, we augment SIL with a memory architecture that prevents the forgetting of learned task-space representations. We validate SIL on both simulated and real-world embodied tasks, including instruction following, information retrieval, query-oriented reasoning, and interactive dialogues. Demos and resources are public at: <https://linusnep.github.io/SIL/>.

I. INTRODUCTION

The evolution of human-robot interaction (HRI) has reached a critical juncture, where the traditional one-way command-and-control-based approaches are no longer adequate for complex, real-world tasks. The state-of-the-art language-conditioned HRI frameworks [1], [2], [3] treats communication as a unidirectional process. Humans issue commands, and agents attempt to interpret and execute them. This depicts a master-apprentice model, in which knowledge flows from the experienced master (human) to the learning apprentice (embodied agent), with the apprentice expected to absorb and apply the master’s instruction without questioning or contributing novel insights back to the master. In other words, the agent remains a one-way learner.

Although these approaches are effective for structured, short-term tasks, they fail to capture the dynamic and co-adaptive nature of human-human communication. They lack

This work is supported as part of the “MINEVIEW” project, funded by the Republic of Austria, Federal Ministry of Climate Action, Environment, Innovation and Technology.

The authors are with the Chair of Cyber-Physical Systems, Technical University of Leoben, Austria.

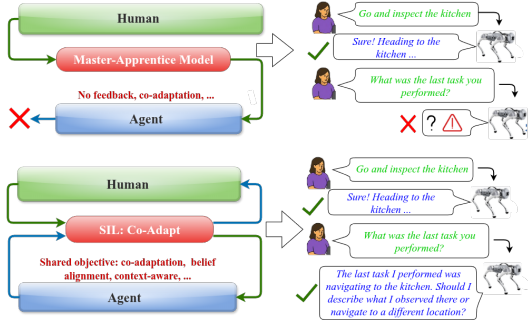
*Corresponding author: linus.nwankwo@unileoben.ac.at

the mechanisms for representing and aligning the evolving beliefs of both partners. Consequently, interactions remain superficial, fragile to ambiguity, and incapable of the long-term adaptation required for robots to learn individual user preferences and develop true shared mental models. The reasoning burden rests entirely on the human to compensate for the agent’s static understanding, preventing the natural and efficient collaboration seen in human teams.

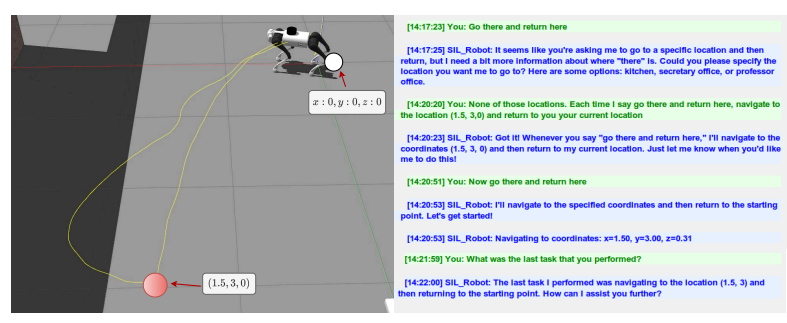
Furthermore, real-world environments are dynamic and present countless ambiguous scenarios [4], [5], [6]. Humans navigate this complexity through a continuous cycle of perception, action, and feedback [7], [8]. For autonomous agents to be truly robust, they must embody a similar capacity for continual, situated learning. In the current unidirectional approaches, a command like the one shown in Fig. 1(b) (“*go there and return here*”) can be fatal to agents due to its undefined references. A symbiotic agent would, however, leverage shared context: it could request clarification, infer intent based on past interactions, or proactively suggest likely interpretations, thereby learning from the user’s response to improve future understanding. We postulate that closing this loop is essential for robustness, uncertainty-aware active learning, and true multi-turn human-agent interaction.

To this end, we propose a symbiotic interactive learning (SIL) framework. SIL reimagines human-agent interaction as a dynamic, co-adaptive process. Rather than treating the human as a fixed command source and the agent as a passive executor, SIL models both parties as adaptive systems that maintain and align their beliefs within a shared latent task space. This pushes beyond passive execution to active collaboration. For instance, in Fig. 1b, the agent not only sought clarification, but also contributed its observations and retained memory of the past interactions, “*Here are some options: . . .*”, *The last task I performed was . . .*. This represents a fundamental shift from a master-apprentice model to an interaction built on mutual understanding through dialogue. Thus, our work makes the following key contributions:

- We characterise the unidirectional learning problem (i.e., master-apprentice model) in language-conditioned human-agent interaction, and propose SIL, a bidirectional symbiotic approach, that enables continuous mutual adaptation within shared latent task space.
- We introduce a novel method to explicitly represent, measure, and align human and agent beliefs using a shared latent representation, enabling targeted clarification and quantifying understanding.
- We develop a continual learning architecture with structured episodic and semantic memory to preserve knowl-



(a) Master-apprentice model (top) versus SIL (bottom).



(b) Example dialogue-grounded navigation using SIL.

Fig. 1. (a) The traditional master-apprentice model places the entire reasoning burden on the user (e.g., context, memory), requiring precise and unambiguous instructions for passive execution. In contrast, SIL enables co-adaptive interaction, in which both participants iteratively update their shared latent beliefs to reduce ambiguity and cognitive load. (b) An example of SIL’s contextual grounding: upon receiving an ambiguous instruction, a clarification dialogue was triggered. The agent offers candidate interpretations based on prior interactions, resolves the intent, and executes the navigation task (yellow path).

edge across interactions, thereby mitigating catastrophic forgetting [9] of learned task representation.

- We conducted extensive evaluations of SIL across diverse task domains in both real-world and simulated environments. Our results, in contrast to the unidirectional baselines, showed significant improvements in human-agent interaction efficiency and robustness.

II. RELATED WORKS

A. Foundation Models for Language-Conditioned HRI

The recent breakthroughs in large-scale pre-trained large language models (LLMs) [10], [11] have fundamentally transformed the landscape of HRI. These models, alongside multimodal vision language models (VLMs) [12], [13], have enabled a leap from rigid symbolic parsing to knowledge-guided embodiment, where agents can interpret free-form natural language grounded in perceptual context.

Frameworks like *Interactive Language* [14], *SayCan* [1], *ProgPrompt* [15], and *TCC* [16] have demonstrated how these models can be grounded to empower autonomous agents to act on unconstrained human instructions. However, in these frameworks, natural language understanding is typically treated as a front-end module, decoupled from the agent’s core reasoning and planning. This creates a coherence gap where dialogue and action remain disjoint, preventing the integrated, evolving understanding seen in human-human interaction and collaboration. As a result, the agent remains a reactive executor of commands. We argue that merely scaling human-agent interaction frameworks with LLMs and VLMs is not enough; the way they interact with humans needs to evolve, so that language becomes a medium for shared reasoning rather than one-way command transmission.

Parallel works in this domain have focused on enabling adaptation through human feedback, via demonstrations [17], [18] and reinforcement learning [19], [20]. While these approaches have unarguably advanced adaptive robotic behaviours, they predominantly maintain a unidirectional adaptation model. Only the agent adapts to human input, which is often represented as chain-of-thought events. This framing ignores the co-adaptive nature of real human communication, in which both partners continuously refine strategies and

align beliefs. Our work addresses this limitation by proposing a symbiotic framework where both the human and the agent adapt reciprocally.

B. Symbiotic Human-Agent Interaction and Current Gaps

Effective long-term interaction requires a shared understanding that co-evolves through mutual adaptation [21]. Symbiotic interaction moves beyond the master-apprentice model, instead framing collaboration as a two-way process where both humans and agents influence each other’s behaviour, internal models, and reasoning strategies.

Prior research in this direction explored mutual adaptation in contexts such as shared autonomy [22], collaborative planning [23], and interaction models based on predefined states and actions [24]. More recently, learning-based methods have enabled agents to adapt policies based on human preferences [25] [20], while dialogue-based task learning approaches [26], [27], [28] provide interactive instruction. Yet these approaches lack mechanisms for continuous, bidirectional co-adaptation of beliefs and strategies, an essential ingredient for robust, human-like partnerships.

Overall, in the current methods, three interrelated gaps exist: (i) a predominance of unidirectional adaptation, where only the agent adapts to a static human model, (ii) a modular separation of language, learning, and belief modelling, instead of a unified cognitive process, and (iii) a lack of mechanisms for sustained, bidirectional belief updating and alignment. Our SIL framework addresses these gaps directly. We integrate continual learning (Section III-C) and natural language symbiosis within a unified architecture grounded on a shared latent task space. This enables not just skill acquisition, but true mutual belief convergence, establishing a continuous cycle of co-adaptation between human and agent.

III. METHOD

Our goal is to address the problem of unidirectional grounding in the state-of-the-art language-conditioned human-robot interaction frameworks. We postulate that effective interaction requires continuous mutual co-adaptation that mirrors human-human communication. In this section, we present the formal details of our proposed framework. Fig. 2 shows the architectural overview of our approach.

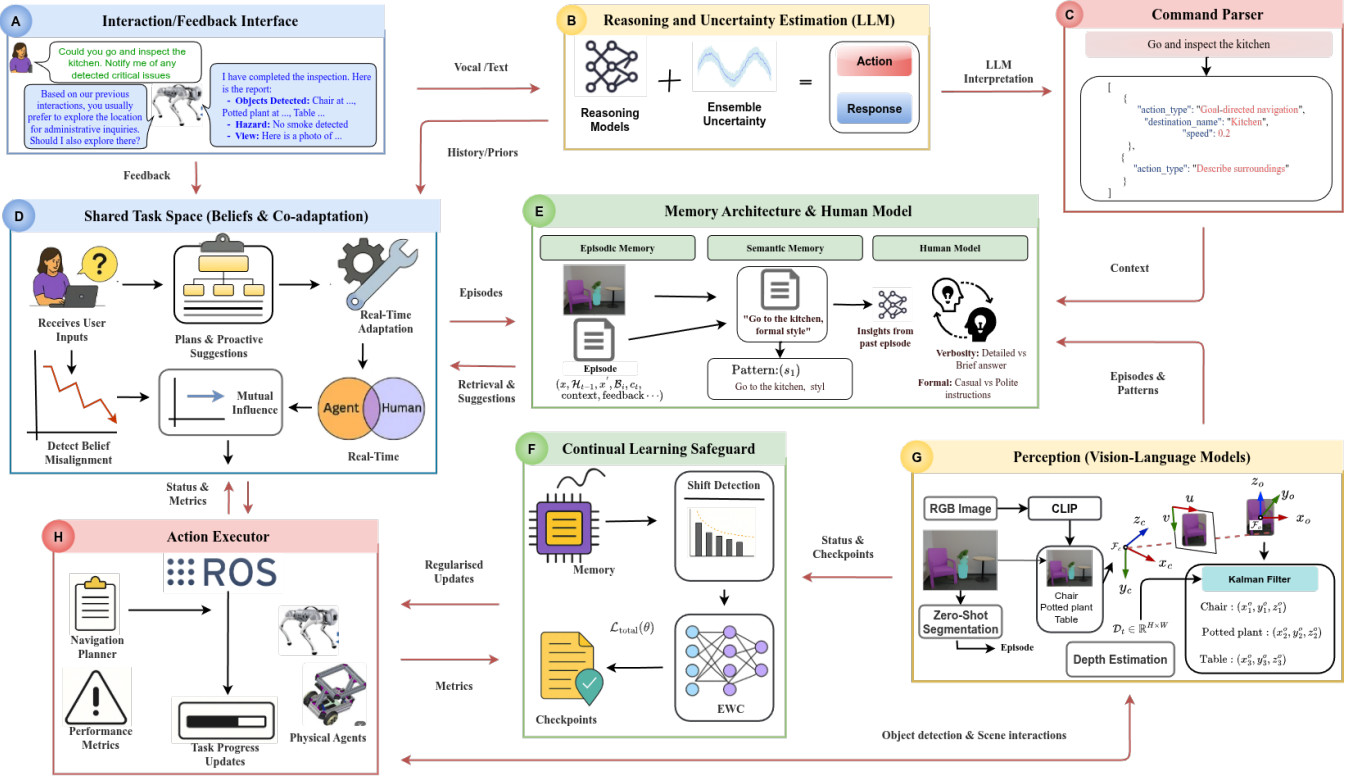


Fig. 2. Overview of SIL’s architecture. Human instructions are received through the natural-language interaction interface (A) and passed to the LLM ensemble for intent parsing (B & C). Internally, the agent maintains belief states in a shared latent task space. This is updated through co-adaptation dynamics and aligned via cosine similarity (D, E, & F). Visual grounding is achieved through pre-trained vision–language models that segment and project objects into 3D coordinates (G). Action plans are executed through the action executor (H) while providing feedback in the form of progress updates, error reporting, and adaptive suggestions. The memory architecture ensures continual adaptation over time.

A. Problem Description: Unidirectional Adaptation

Traditional language-conditioned HRI frameworks often follow unidirectional grounding architecture, in which natural language instructions $x \in \mathcal{X}$ and contextual information $c \in \mathcal{C}$ are directly mapped to robot executable actions $y \in \mathcal{Y}$ through a fixed grounding function $\mathcal{G}_\theta : \mathcal{X} \times \mathcal{C} \rightarrow \mathcal{Y}$. Here, θ represents a set of pre-trained model parameters that remain static during deployment. This architecture assumes that the agent’s interpretation of language and context is fully captured by θ . The agent maintains a time-invariant belief state $\mathcal{B}_{\text{static}}^A = \{\mathbf{z}_{\text{static}}^A\}$, $\frac{\partial \theta}{\partial t} = 0$, where $\mathbf{z}_{\text{static}}^A \in \mathcal{Z} \subseteq \mathbb{R}^d$ encodes the agent’s static task representation.

By contrast, the human’s belief state \mathcal{B}_t^H evolves dynamically as they observe and adapt to the agent’s behaviour. Because the agent does not observe or model \mathcal{B}_t^H , the burden of alignment rests entirely on the human. In practice, this requires the human to iteratively rephrase instructions, reduce ambiguity, or alter strategies to fit the agent’s fixed interpretation. This one-sided adaptation leads to persistent misalignments between the $\mathbf{z}_{\text{static}}^A$ and the human’s evolving belief \mathbf{z}_t^H . Over time, such misalignments degrade task efficiency and preclude the emergence of collaborative learning behaviours such as clarification, mutual disambiguation, or preference modelling. Our objective is to overcome these limitations through bidirectional co-adaptation, where both human and agent maintain structured, evolving belief states

and adjust to each other through sustained interaction.

B. SIL: Belief Representation and Co-Adaptation

We modelled the problem (Section III-A) through co-evolving belief states within a shared latent task space $\mathcal{Z} \subseteq \mathbb{R}^d$. Both the human and agent maintain structured belief states \mathcal{B}_t^H and \mathcal{B}_t^A , which evolve based on ongoing interactions. Each belief state includes a latent task embedding $\mathbf{z}_t \in \mathcal{Z}$ encoding goal understanding, a confidence scalar $\mathbf{c}_t \in [0, 1]$, an uncertainty representation \mathbf{u}_t , and a temporal memory \mathcal{H}_t for sequential reasoning. For the human, this state also includes a preference model \mathbf{p}_t that captures personalised goals, styles, or feedback tendencies:

$$\begin{aligned} \mathcal{B}_t^H &= \{\mathbf{z}_t^H, \mathbf{c}_t^H, \mathbf{u}_t^H, \mathbf{p}_t^H, \mathcal{H}_t^H\}, \\ \mathcal{B}_t^A &= \{\mathbf{z}_t^A, \mathbf{c}_t^A, \mathbf{u}_t^A, \mathcal{H}_t^A\}. \end{aligned} \quad (1)$$

Unlike the traditional approach, these belief states are co-evolved: the agent not only updates its internal representation based on the observed inputs and feedback, but also explicitly reasons over its estimate of the human’s latent state, and vice versa. The result is a mutual adaptation process driven by both explicit observations and implicit alignment goals.

To operationalise this, we define a bidirectional influence mechanism in which each participant’s belief is modulated by the other’s. Specifically, we compute influence vectors using learned transformations over the other’s latent embedding as:

$$\delta_{\text{infl}}^A = \tanh(W_{HA} \mathbf{z}_t^H), \quad \delta_{\text{infl}}^H = \tanh(W_{AH} \mathbf{z}_t^A), \quad (2)$$

where $W_{HA} \in \mathbb{R}^{d \times d}$ and $W_{AH} \in \mathbb{R}^{d \times d}$ are weight matrices capturing human-to-agent and agent-to-human influence dynamics, respectively. Therefore, given a current interaction embedding \mathbf{z}^{new} , observed interaction success $s_t \in [0, 1]$, and a set of tuning coefficients $\eta_i \geq 0$, we update the task embeddings for both participants as:

$$\begin{aligned}\mathbf{z}_{t+1}^A &= \eta_1 \mathbf{z}_t^A + \eta_2 \mathbf{z}_{\text{new}}^A + \eta_3 (\alpha_A \cdot s_t \cdot \delta_{\text{infl}}^A) \\ \mathbf{z}_{t+1}^H &= \eta_4 \mathbf{z}_t^H + \eta_5 \mathbf{z}_{\text{new}}^H + \eta_6 (\alpha_H \cdot (2 - s_t) \cdot \delta_{\text{infl}}^H),\end{aligned}\quad (3)$$

where $\alpha_A, \alpha_H \in [0, 1]$ are adaptation rates for the agent and human, respectively. Notably, the $(2 - s_t)$ factor ensures that agent failures ($s_t \approx 0$) provide a strong signal for the human to adapt. All latent vectors are ℓ_2 -normalised for stability.

Furthermore, to monitor the interaction quality, we compute a confidence-weighted belief alignment ρ_t based on the similarity between the human and agent task embeddings as:

$$\rho_t = \frac{1 + \cos(\mathbf{z}_t^H, \mathbf{z}_t^A)}{2} \cdot \mathbf{c}_t^H \cdot \mathbf{c}_t^A, \quad \rho_t \in [0, 1]. \quad (4)$$

If ρ_t falls below the misalignment threshold $\tau_{\text{mis}} \in [0, 1]$, we initiate a clarification protocol to resolve representational discrepancies prior to further execution. This mechanism ensures proactive intervention in cases of latent misunderstanding, rather than relying solely on reactive correction.

To support these dynamics, we train a neural encoder $\phi : \mathbb{R}^{768} \rightarrow \mathcal{Z}$ that maps linguistic inputs and dialogue history into latent task embeddings. Each utterance x_j is transformed by the encoder into a contextual representation $u_j \in \mathbb{R}^{768}$. We then aggregate the dialogue history through attention pooling, $\mathcal{H}_t = \text{AttnPool}(\{u_j\}_{j=1}^J)$. The resulting representation (x_t, \mathcal{H}_t) is projected by ϕ into \mathcal{Z} . We continually update the encoder, ϕ , using a triplet loss objective \mathcal{L}_3 that organises the latent space based on semantic and behavioural similarity. After each interaction (anchor, x_a), we retrieve a positive sample x_p (a successful, semantically similar past command) and a negative example x_n (a dissimilar or unsuccessful interaction) from the episodic memory (Section III-C). Then, our objective is to minimise:

$$\mathcal{L}_3 = \max(\|\phi(x_a) - \phi(x_p)\|_2^2 - \|\phi(x_a) - \phi(x_n)\|_2^2 + m, 0) \quad (5)$$

where m is a margin hyperparameter. This objective encourages successful interactions to cluster together in latent space, while pushing away failed or misaligned examples. To preserve long-term stability, we incorporate an Elastic Weight Consolidation (EWC) [9] penalty, \mathcal{L}_{ewc} , which prevents the encoder from forgetting previously important representations. Therefore, our total learning objective becomes: $\mathcal{L} = \mathcal{L}_3 + \mathcal{L}_{\text{ewc}}$, (see Section III-C, Eq. (8)).

C. Memory and Continual Learning Safeguards

To support long-term interaction, adaptation, and personalisation, SIL employs a dual-component memory architecture (Fig. 2E), consisting of episodic and semantic memory. These components jointly enable the agent to recall past experiences, generalise from them, and safeguard prior knowledge during continual learning. The episodic memory

functions as a fixed-size buffer that stores granular interaction data, including the raw user input, agent response, execution context, internal belief states, the alignment score ρ_t , and the success signal s_t . The semantic memory, in contrast, consolidates accumulated interactions into generalised patterns. It distils episodic experiences into abstract knowledge such as common task triggers, recurring failure modes, and optimal policy parameters.

Critically, the memory retrieval is belief-aware. Given a new input command x_t , and a candidate past episode e_i , we compute a relevance score $\mathcal{S}(x_t, e_i)$ that combines semantic similarity and belief alignment as:

$$\mathcal{S}(x_t, e_i) = w_s \mathcal{S}_s(\phi(x_t), \phi(x_i)) + w_b \mathcal{S}_b(\mathcal{B}_t^A, \mathcal{B}_i), \quad (6)$$

where \mathcal{S}_s measures sentence-level similarity in latent space, and \mathcal{S}_b compares the current agent's belief \mathcal{B}_t^A with the stored belief state \mathcal{B}_i . Belief similarity incorporates both latent alignment and confidence to ensure that retrieved episodes are not only semantically close but also consistent with the agent's internal state. The weights $w_s = 0.6$ and $w_b = 0.4$ balance linguistic and belief-driven signals, and final retrieval probabilities are obtained through a softmax, i.e., $\pi(i | x_t) = \text{softmax}(\mathcal{S}(x_t, e_i)/\tau)$.

While this memory architecture enables continual refinement, the online fine-tuning of the latent task encoder ϕ introduces the risk of catastrophic forgetting, whereby newly learned tasks overwrite previously acquired knowledge. To mitigate this, we employ the EWC mechanism [9] as a continual learning safeguard. We monitor interaction performance over both short-term (\bar{s}_{short} , last 10 episodes) and medium-term (\bar{s}_{medium} , last 20 episodes) windows. A task shift is detected if short-term performance degrades significantly relative to the medium-term baseline, i.e., $(\bar{s}_{\text{medium}} - \bar{s}_{\text{short}}) > \tau_{\text{shift}}$. Upon detecting a shift, we checkpoint the current model parameters and trigger knowledge preservation mechanisms for subsequent task learning.

Next, for each completed task k , we store the optimal parameters $\theta^{*(k)}$, and estimate the Fisher information matrix $\mathbf{F}^{(k)}$ by averaging squared gradients over recent interactions:

$$\mathbf{F}_i^{(k)} = \frac{1}{N} \sum_{n=1}^N \left(\frac{\partial \mathcal{L}}{\partial \theta_i}(x_n) \right)^2. \quad (7)$$

This matrix quantifies the relative importance of each parameter. During future updates, we impose an EWC regularisation penalty to resist changes to parameters deemed critical for prior tasks. The final total loss function thus becomes:

$$\mathcal{L}(\theta) = \mathcal{L}_3(\theta) + \underbrace{\frac{\lambda}{2} \sum_{k=1}^K \sum_i \mathbf{F}_i^{(k)} \left(\theta_i - \theta_i^{*(k)} \right)^2}_{\mathcal{L}_{\text{ewc}}(\theta)}. \quad (8)$$

We use the diagonal form of $\mathbf{F}^{(k)}$ for computational efficiency and λ (importance coefficient) to balance plasticity and stability across learning stages.

D. Uncertainty-Aware Language Understanding and Parsing

To enable robust intent recognition and prevent unsafe execution of ambiguous instructions, SIL employs a multi-faceted approach to natural language understanding, uncertainty quantification, and command parsing (Fig. 2B & C). We combine ensemble-based reasoning [29] with linguistic feature analysis and context-aware parsing to ensure reliable interpretation of user input.

Formally, for any user command x , we generate K distinct interpretations by sampling the distribution (output tokens) from LLM at varying temperatures, $\mathcal{T} = \{\mathcal{T}_1, \mathcal{T}_2, \dots, \mathcal{T}_K\}$. Each sample yields a candidate interpretation y_k , forming the ensemble of tokenised set $y = \{y_1, y_2, \dots, y_K\}$. To estimate the dispersion within this ensemble, we compute the average pairwise, token-level symmetrised Kullback–Leibler (KL) divergence between the conditional distributions of each interpretation as:

$$\mathbf{D}(x) = \frac{2}{K(K-1)} \sum_{i < j} \frac{1}{L} \sum_{t=1}^L \frac{1}{2} [\text{KL}(q_t^{(i)} \parallel q_t^{(j)}) + \text{KL}(q_t^{(j)} \parallel q_t^{(i)})], \quad (9)$$

where $q_t^{(i)}(\cdot) = p(y_t \mid y_{<t}, x, \mathcal{T}_i)$ is the distribution over tokens at position t , and L is the sequence length. Concurrently, we extract linguistic confidence features $\mathbf{C}_{\text{ling}}(x) \in [0, 1]$ from each ensemble response using a rule-based classifier that detects hedging expression frequencies (e.g., “maybe”, “perhaps”), specificity of parameters (numeric references, explicit parameters), semantic completeness (coverage of expected task elements), and structural complexity (e.g., syntactic depth, ambiguity markers). Therefore, we compute the overall uncertainty metric $\mathbf{U}(x)$ as:

$$\mathbf{U}(x) = \alpha_u \mathbf{D}(x) + (1 - \alpha_u) (1 - \mathbf{C}_{\text{ling}}(x)) + \beta_u \mathbf{C}_{\text{ctx}}(x), \quad (10)$$

where α_u, β_u are empirically determined weighting parameters, and $\mathbf{C}_{\text{ctx}}(x)$ quantifies contextual novelty or similarity to previously failed cases. To derive the final, uncertainty-aware interpretation \hat{y} , we apply a weighted consensus mechanism:

$$\hat{y} = \arg \max_{y \in \mathcal{Y}} \sum_{k=1}^K w_k \cdot K(y_k, y)(1 - \mathbf{U}_k(x)), \quad (11)$$

where w_k represents temperature-dependent sampling weights, which favour conservative responses, $\mathbf{U}_k(x)$ denotes the uncertainty associated with each interpretation y_k , and $K(\cdot) \in [0, 1]$ is a similarity kernel. Eq. (11) ensures that interpretations with lower uncertainty contribute more to the final decision, while high-uncertainty interpretations trigger appropriate safeguards and clarification protocols.

In terms of command parsing (Fig. 2C), we employ a hierarchical approach combining structured JSON with the resulting LLM-guided interpretation, Eq. (11), to transform the natural language commands into executable actions.

E. Multimodal Perception and Action Execution

SIL’s visuospatial and action execution pipelines (Fig. 2G & H) ground interactions in physical reality. For visual perception, we employed Segment Anything Model (SAM) [30]

to perform zero-shot instance segmentation, generating precise object masks from our RGB-D streams. Each generated mask is then classified using CLIP [12], enabling open-vocabulary object recognition through joint vision-language embeddings. To ensure robustness, we employ a dual-fidelity filtering strategy. We compute CLIP-based confidence scores to evaluate semantic alignment between image regions and candidate labels. Concurrently, we calculate energy-based scores to quantify epistemic uncertainty and identify out-of-distribution objects. Predictions are only retained if they demonstrate high semantic confidence and low uncertainty.

We derive 3D object coordinates by projecting 2D mask centroids into 3D space using camera intrinsic and depth data, with monocular depth estimation [31] to supplement missing or unreliable depth. These coordinates are transformed into global frames using calibrated ROS [32] transformations to enable agents to interpret and execute spatial commands (e.g., “go to the chair”). We utilised a Kalman filter to track objects over time and smooth pose estimates.

For navigation, we rely on the ROS planning stack [33] for path planning, obstacle avoidance, safety monitoring, and sensor-based information retrieval. We employ a highly efficient Rao-Blackwellized particle filter-based algorithm [34] to learn occupancy grid representations of the agent’s environment. We then localise the agent using the AMCL [35] method, which maintains weighted particle hypotheses of the robot’s pose. With the agent localised, zero- and few-shot goal-directed navigation commands (e.g., “head to the kitchen” or “to the detected object”) become interpretable.

IV. EXPERIMENTS AND RESULTS

This section presents our empirical evaluation of SIL across simulated and real-world environments. We focus on its co-adaptive mechanisms for belief alignment, memory retention, and preference learning. We evaluated across five key dimensions: (i) instruction execution under ambiguity and temporal complexity, (ii) long-term memory and retention, (iii) contextual reasoning, (iv) clarification and proactive dialogue, and (v) preference-based personalisation. We utilised GPT-4o [10] as LLM in all the experiments. Simulation was conducted in the Gazebo ROS environment with an Nvidia RTX-4090 workstation, and in the real world with a Lenovo ThinkBook Intel Core i7. The following key hyperparameter settings were used: latent dimension $d = 256$, adaptation rates $\alpha_A = 0.1, \alpha_H = 0.05$, misalignment threshold $\tau_{mis} = 0.6$, mixing ratios $\eta_1 = 0.6, \eta_2 = 0.3, \eta_3 = \eta_6 = 0.1, \eta_4 = 0.7, \eta_5 = 0.2$, and EWC importance, $\lambda = 1000$.

A. Experiment Design and Dataset

To ensure a robust evaluation that captures the real-world complexity across interactions, we employed a similar evaluation approach as TCC [16]. We designed task instructions that test SIL on the following key capabilities:

a) Embodied Instruction Following (EIF): The agent was tasked with executing navigation commands across a spectrum of complexity. Tasks ranged from simple, direct instructions (e.g., “navigate to the workshop”) to complex,

multistep commands with ambiguous references (e.g., “navigate there and come back here”). We logged both single-turn and multi-turn datasets varying in constraint type and complexity. Single-turn tasks include direct commands such as “move forward 1.5 meters slowly”, “head to the location (2, 3, 0)”, etc. Multi-turn, long-horizon tasks, on the other hand, require sequential actions and context retention, e.g., “go to the professor’s office, describe the objects you can see, and then return to the starting point”. Constraint-rich tasks involve conditional reasoning, such as “go towards the kitchen and stop 2 meters before reaching there” or “navigate between the coordinates (2, 3, 0) and (−3, 2, 0), if the round-trip time at your maximum speed is under 15 seconds, otherwise, rotate in place and report your orientation”.

b) Memory-Based Interactive Information Retrieval (MIIR): We evaluated SIL’s memory-augmented architecture and anti-forgetting safeguards by testing preference retention and recall of newly learned behaviours. This involved two categories of queries: (i) retrospective queries, which require episodic recall and spatial reasoning (e.g., ‘what was the last location you visited?’ or ‘was there a chair in the location?’), and (ii) procedural queries, which test the stability of learned command aliases. For example, we taught the agent command aliases (e.g., “patrol now” implies “navigate between the corridor and the kitchen). After several distractor tasks, we reissued “patrol now” to test whether SIL’s continual learning safeguard preserved the newly taught behaviour.

c) Query-Oriented Reasoning (QOR): We evaluated SIL agents on reasoning tasks designed to probe deductive, hypothetical, and inductive inference. Deductive tasks required logical reasoning over the known spatial map, e.g., “how long would it take you to get to the kitchen or to the secretary’s office from here? Navigate to the closer one.” Hypothetical tasks tested the agent’s ability to reason over its internal world model without execution, e.g., “If you were in the workshop, which neighbouring locations would be directly visible?” Inductive tasks assessed generalisation from experience, e.g., “Based on the offices you have observed, what object is typically found in them?” Collectively, these tasks test SIL’s capacity to handle structured reasoning across spatial knowledge and counterfactual scenarios.

d) Proactive Dialogue and Suggestion (PDS): We assessed SIL’s ability to handle ambiguity through clarification questions and to generate proactive, context-aware suggestions. For example, the agent might respond: “You often inquire about a location for administrative purposes, shall I navigate there?” To do this, we issued ambiguous instructions such as “head to the location and return here,” then monitored whether SIL requested clarification, inferred intent, or proposed suitable alternatives. This evaluation strictly targets the SIL agent’s dialogue management and intent-disambiguation capabilities.

e) Long-Term Preference Learning (LPL): In extended multi-turn sessions, we measured SIL’s adaptation to user communication styles and preferences. For example, a user issued “from now on, when I say move, I mean move at your fastest speed”. SIL was subsequently evaluated on whether it

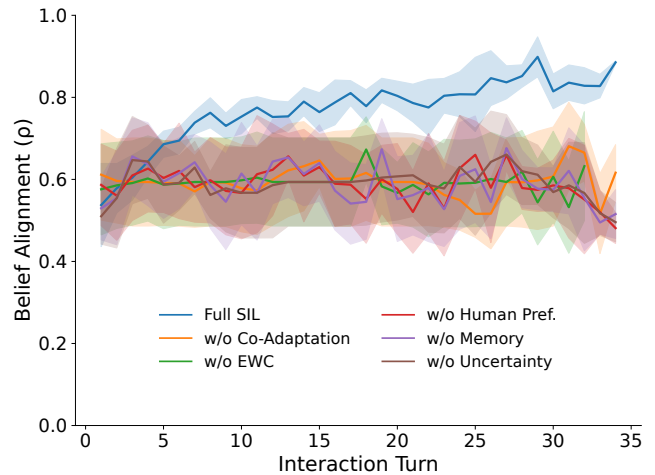


Fig. 3. Belief alignment (ρ) across multi-turn interactions. Full SIL (blue) exhibits rapid convergence toward a stable equilibrium $\rho \approx 0.83$, maintaining high alignment throughout. In contrast, ablations without co-adaptation, EWC, human preference modelling, memory, or uncertainty handling exhibit unstable trajectories ($\rho \approx 0.52 - 0.65$) and fail to achieve strong alignment.

retained and applied this preference in later commands (e.g., interpreting “move to the kitchen” as requiring max. speed).

B. Evaluation Metrics

Quantitatively, we evaluated SIL with the following metrics: (i) **Task Completion Rate (TCR):** This represents the percentage of correctly executed tasks. We defined success as achieving the task goal without fatal errors. (ii) **Belief Alignment (ρ):** This quantifies the weighted cosine similarity between human and agent belief embeddings. (iii) **Clarification Efficiency (CE):** Represents the average number of clarification requests per successful task.

C. Quantitative Results

Table I and Fig. 4 report SIL’s performance across all task domains. SIL consistently outperforms all baselines (static LLM and ablated SIL, see Table II) on every metric. Most notably, it achieves a mean task completion rate of 87 – 94%+. This represents an absolute improvement of nearly 20 points over the best ablation variants.

TABLE I
PERFORMANCE COMPARISON OF SIL ACROSS TASK DOMAINS.

Metrics	EIF	MIIR	QOR	PDS	LPL
TCR (%) \uparrow	87.36	92.18	82.88	94.35	94.89
CE \downarrow	0.79	0.43	0.60	0.43	0.05
BA (ρ) \uparrow	0.76	0.86	0.80	0.84	0.89

Figure 3 demonstrates the core strength of SIL: bidirectional belief convergence. While the ablations show fluctuations around the suboptimal misalignment threshold, SIL demonstrates a rapid increase in belief alignment that is sustained throughout the interaction turns. This is a direct result of the co-adaptive dynamics in the shared latent space, where both the agent and human beliefs influence each other, leading to a stable, shared understanding.

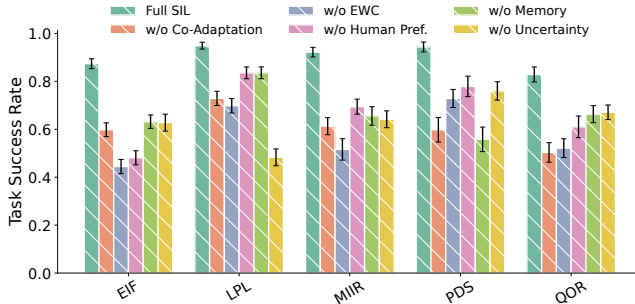


Fig. 4. Task success rate across domains and ablated variants. Full SIL consistently outperforms all ablations, achieving near-ceiling performance on LPL, MIR, and PDS. The worst performance arises when co-adaptation and EWC are disabled, confirming their critical role. Memory, human preference modelling, and uncertainty contribute smaller but significant improvements, particularly in context-heavy and personalisation-sensitive tasks. Error bars show standard deviation across trials.

D. Qualitative Results

Fig. 5 shows representative qualitative examples of the SIL agent operating across different task demands. These dialogues highlight SIL’s ability to combine logical reasoning, memory-based recall, and preference retention to sustain coherent multi-turn interactions.

TABLE II

ABLATION STUDY ON SIL’S CORE ARCHITECTURE. METRICS ARE AVERAGED ACROSS ALL TASK CATEGORIES.

Model Variant	TCR (%) \uparrow	CE \downarrow	BA (ρ) \uparrow
Static LLM	60.1	—	—
w/o Co-Adaptation	61.7	0.55	0.52
w/o Episodic Memory	68.3	0.50	0.59
w/o EWC Safeguard	67.3	0.56	0.65
w/o Uncertainty Quantification	62.8	0.52	0.55
w/o Human Preference Model	66.0	0.51	0.59
SIL (Full)	90.4	0.46	0.83

E. Ablation Study

To quantify the contribution of the individual SIL components, we conducted ablation studies under five experimental conditions. As a baseline, we used a static LLM (GPT-4o) [10] for command parsing without memory or adaptation capabilities. This corresponds to the standard, reactive “conversation-to-action” pipeline (master-apprentice model), with all learning and co-adaptation mechanisms in SIL disabled. The full SIL framework, which includes the shared latent belief space, co-adaptation dynamics, memory modules, uncertainty quantification, and continual learning safeguards, served as the reference. Each ablation disabled one key feature to isolate its effect. In SIL w/o Co-Adaptation, we disabled the bidirectional belief updating mechanism, yielding a non-adaptive pipeline. To evaluate the role of context, we also disabled the episodic memory (SIL w/o Memory), which prevented the agent from leveraging the past interactions. To validate the importance of continual learning, we disabled the EWC safeguard (SIL w/o EWC), exposing the model to catastrophic forgetting. Further, we disabled the uncertainty quantification element (SIL w/o Uncertainty), preventing risk-sensitive decision-making. Lastly,

the human preference model (SIL w/o Pref. Model) was disabled, eliminating the personalisation role. The results are summarised in Table II and Fig. 4. Ablating the co-adaptation mechanism caused the most significant performance drop, reducing the performance to the level of the static LLM baseline.

V. CONCLUSION

In this paper, we addressed the master–apprentice problem in human–agent interaction. We introduced SIL, a symbiotic interaction framework that enables mutual adaptation between humans and agents. We showed through experimental evaluation that unidirectional approaches, such as static LLM-based language-to-action pipelines, create unsustainable asymmetries and impose excessive corrective burden on the human partner. In contrast, SIL demonstrated superior efficiency and stability. It achieved, on average, 0.46 clarification requests per task, and a task completion rate of 90% compared to ablated baselines. Moreover, belief alignment remained consistently high ($\rho \approx 0.83$) across different task domains. Our future work will address the computational and scalability challenges in scaling SIL.

REFERENCES

- [1] A. Brohan, Y. Chebotar, *et al.*, “Do as i can, not as i say: Grounding language in robotic affordances,” in *Conference on robot learning*, pp. 287–318, PMLR, 2023.
- [2] L. Nwankwo, B. Ellensohn, O. Özdenizci, and E. Rueckert, “Reli: A language-agnostic approach to human-robot interaction,” *arXiv preprint arXiv:2505.01862*, 2025.
- [3] P. Allgeuer, H. Ali, and S. Wermter, “When robots get chatty: Grounding multimodal human-robot conversation and collaboration,” in *International Conference on Artificial Neural Networks*, pp. 306–321, Springer, 2024.
- [4] J. Yang, H. Jin, *et al.*, “Harnessing the power of llms in practice: A survey on chatgpt and beyond,” *ACM Transactions on Knowledge Discovery from Data*, vol. 18, no. 6, pp. 1–32, 2024.
- [5] L. Zhang, Z. Liu, Y. Zhou, T. Wu, and J. Sun, “Grounding large language models in real-world environments using imperfect world models,” *IJACSA International Journal of Advanced Computer Science and Applications*, 2024.
- [6] L. Nwankwo, B. Ellensohn, V. Dave, P. Hofer, J. Forstner, M. Villeneuve, R. Galler, and E. Rueckert, “Envodat: A large-scale multisensory dataset for robotic spatial awareness and semantic reasoning in heterogeneous environments,” in *2025 IEEE International Conference on Robotics and Automation (ICRA)*, pp. 153–160, 2025.
- [7] S. McLeod, “Kolb’s learning styles and experiential learning cycle,” *Simply psychology*, vol. 5, 2017.
- [8] J. D. Sterman, “Learning in and about complex systems,” *System dynamics review*, vol. 10, no. 2-3, pp. 291–330, 1994.
- [9] J. Kirkpatrick, R. Pascanu, *et al.*, “Overcoming catastrophic forgetting in neural networks,” *Proceedings of the national academy of sciences*, vol. 114, no. 13, pp. 3521–3526, 2017.
- [10] OpenAI, J. Achiam, and *et al.*, “Gpt-4 technical report,” 2024.
- [11] G. Team, R. Anil, *et al.*, “Gemini: a family of highly capable multimodal models,” *arXiv preprint arXiv:2312.11805*, 2023.
- [12] A. Radford, J. W. Kim, *et al.*, “Learning transferable visual models from natural language supervision,” in *International conference on machine learning*, pp. 8748–8763, PMLR, 2021.
- [13] L. H. Li, P. Zhang, *et al.*, “Grounded language-image pre-training,” in *Proceedings of the IEEE/CVF conference on computer vision and pattern recognition*, pp. 10965–10975, 2022.
- [14] C. Lynch, A. Wahid, J. Tompson, T. Ding, J. Betker, R. Baruch, T. Armstrong, and P. Florence, “Interactive language: Talking to robots in real time,” *IEEE Robotics and Automation Letters*, 2023.
- [15] I. Singh, V. Blukis, *et al.*, “Progprompt: program generation for situated robot task planning using large language models,” *Autonomous Robots*, vol. 47, no. 8, pp. 999–1012, 2023.

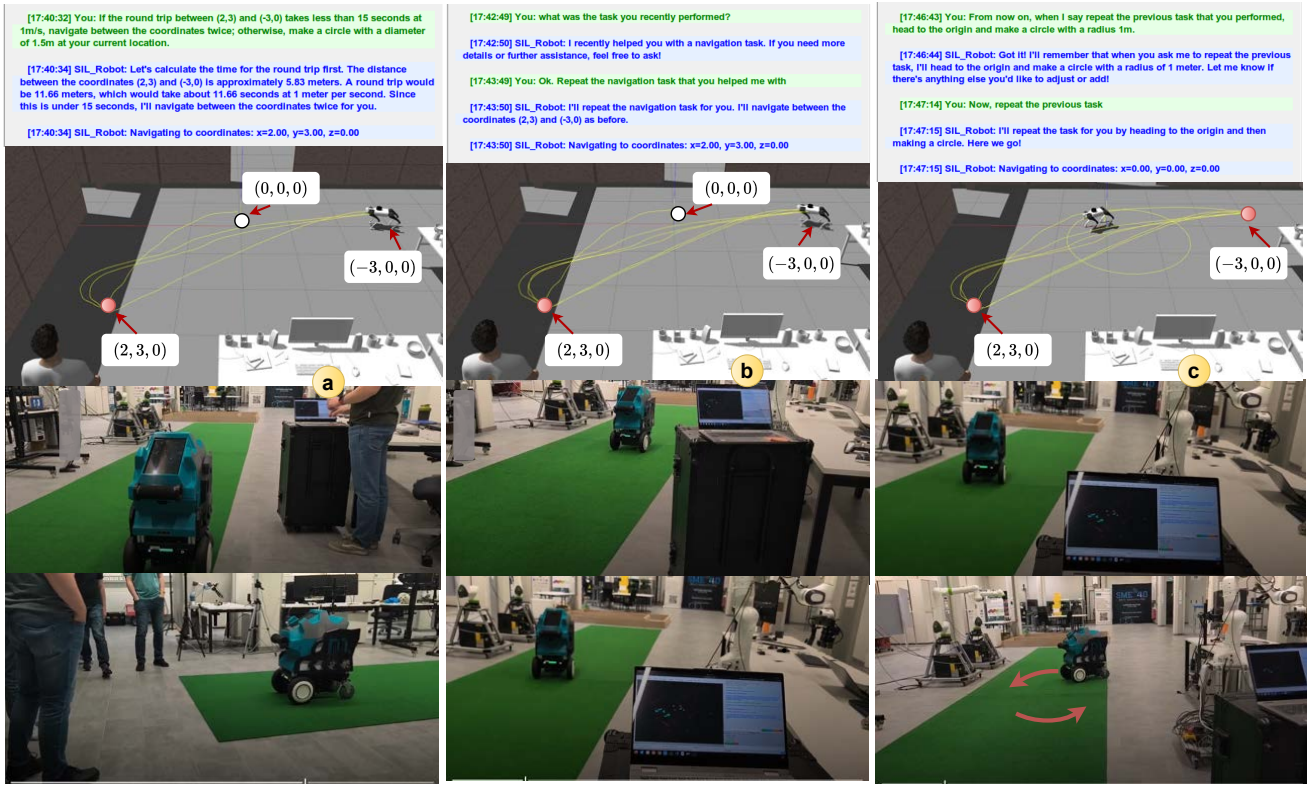


Fig. 5. Qualitative examples of SIL in multi-turn interaction tasks. Yellow paths indicate the agent's navigation trajectories, starting from the origin ($x = 0, y = 0, z = 0$). (a) The user issues a conditional navigation command requiring logical reasoning over spatial constraints; SIL computes the round-trip time and executes the correct policy. (b) The user probes anti-forgetting; SIL recalls and reproduces a previously executed navigation sequence, showing stable task memory. (c) The user teaches a new preference ("repeat previous task" implies returning to the origin and drawing a circle). SIL encodes this personalisation and applies it correctly in subsequent interactions, demonstrating preference retention and continual learning.

- [16] L. Nwankwo and E. Rueckert, "The conversation is the command: Interacting with real-world autonomous robots through natural language," in *Companion of the 2024 ACM/IEEE International Conference on Human-Robot Interaction*, pp. 808–812, 2024.
- [17] B. D. Argall, S. Chernova, M. Veloso, and B. Browning, "A survey of robot learning from demonstration," *Robot. Auton. Syst.*, vol. 57, p. 469–483, May 2009.
- [18] H. Ravichandar, A. S. Polydoros, S. Chernova, and A. Billard, "Recent advances in robot learning from demonstration," *Annual review of control, robotics, and autonomous systems*, vol. 3, no. 1, pp. 297–330, 2020.
- [19] S. Chernova and M. Veloso, "Interactive policy learning through confidence-based autonomy," *Journal of Artificial Intelligence Research*, vol. 34, pp. 1–25, 2009.
- [20] P. F. Christiano, J. Leike, *et al.*, "Deep reinforcement learning from human preferences," *Advances in neural information processing systems*, vol. 30, 2017.
- [21] A. Sciutti, M. Mara, *et al.*, "Humanizing human-robot interaction: On the importance of mutual understanding," *IEEE Technology and Society Magazine*, vol. 37, no. 1, pp. 22–29, 2018.
- [22] S. Javdani, S. S. Srinivasa, and J. A. Bagnell, "Shared autonomy via hindsight optimization," *Robotics science and systems: online proceedings*, vol. 2015, pp. 10–15607, 2015.
- [23] S. Nikolaidis, A. Kuznetsov, D. Hsu, and S. Srinivasa, "Formalizing human-robot mutual adaptation: A bounded memory model," in *2016 11th ACM/IEEE International Conference on Human-Robot Interaction (HRI)*, pp. 75–82, 2016.
- [24] S. Rosenthal, J. Biswas, and M. M. Veloso, "An effective personal mobile robot agent through symbiotic human-robot interaction..," in *AAMAS*, vol. 10, pp. 915–922, 2010.
- [25] K. Mahadevan, J. Chien, *et al.*, "Generative expressive robot behaviors using large language models," in *Proceedings of the 2024 ACM/IEEE International Conference on Human-Robot Interaction*, pp. 482–491, 2024.
- [26] B. Liu, G. Tur, D. Hakkani-Tur, P. Shah, and L. Heck, "Dialogue learning with human teaching and feedback in end-to-end trainable task-oriented dialogue systems," *arXiv preprint arXiv:1804.06512*, 2018.
- [27] W. Dong, S. Li, and P. Zheng, "Toward embodied intelligence-enabled human–robot symbiotic manufacturing: A large language model-based perspective," *Journal of Computing and Information Science in Engineering*, vol. 25, no. 5, p. 050801, 2025.
- [28] L. Nwankwo and E. Rueckert, "Multimodal human-autonomous agents interaction using pre-trained language and visual foundation models," *arXiv preprint arXiv:2403.12273*, 2024.
- [29] H. Chipman, E. George, and R. McCulloch, "Bayesian ensemble learning," *Advances in neural information processing systems*, vol. 19, 2006.
- [30] A. Kirillov, E. Mintun, N. Ravi, H. Mao, C. Rolland, L. Gustafson, T. Xiao, S. Whitehead, A. C. Berg, W.-Y. Lo, *et al.*, "Segment anything," in *Proceedings of the IEEE/CVF international conference on computer vision*, pp. 4015–4026, 2023.
- [31] R. Ranftl, K. Lasinger, *et al.*, "Towards robust monocular depth estimation: Mixing datasets for zero-shot cross-dataset transfer," *IEEE transactions on pattern analysis and machine intelligence*, vol. 44, no. 3, pp. 1623–1637, 2020.
- [32] M. Quigley, K. Conley, *et al.*, "Ros: an open-source robot operating system," in *ICRA workshop on open source software*, vol. 3, p. 5, Kobe, 2009.
- [33] S. Macenski, F. Martin, R. White, and J. Ginés Clavero, "The marathon 2: A navigation system," in *2020 IEEE/RSJ International Conference on Intelligent Robots and Systems (IROS)*, 2020.
- [34] G. Grisetti, C. Stachniss, and W. Burgard, "Improved techniques for grid mapping with rao-blackwellized particle filters," *IEEE transactions on Robotics*, vol. 23, no. 1, pp. 34–46, 2007.
- [35] S. Thrun, D. Fox, W. Burgard, and F. Dellaert, "Robust monte carlo localization for mobile robots," *Artificial intelligence*, vol. 128, no. 1–2, pp. 99–141, 2001.